ACS APPLIED MATERIALS & INTERFACES

Research Article

www.acsami.org

Suppression of Copper Thin Film Loss during Graphene Synthesis

Alvin L. Lee, Li Tao, and Deji Akinwande*

Microelectronics Research Center, Department of Electrical and Computer Engineering, The University of Texas at Austin, Austin, Texas 78758, United States

Supporting Information

ABSTRACT: Thin metal films can be used to catalyze the growth of nanomaterials in place of the bulk metal, while greatly reducing the amount of material used. A big drawback of copper thin films (0.5−1.5 μm thick) is that, under high temperature/vacuum synthesis, the mass loss of films severely reduces the process time due to discontinuities in the metal film, thereby limiting the time scale for controlling metal grain and film growth. In this work, we have developed a facile method, namely "covered growth" to extend the time copper thin films can be exposed to high temperature/vacuum environment for graphene synthesis. The key to preventing severe mass loss of copper film during the high temperature chemical vapor deposition (CVD) process is to have a cover piece on top of the growth substrate. This new "covered growth" method enables the high-temperature annealing of the copper film upward of 4 h with minimal mass loss, while increasing copper film grain and graphene domain size. Graphene was then successfully grown on the capped copper film with subsequent transfer for device fabrication. Device characterization indicated equivalent physical, chemical, and electrical properties to conventional CVD graphene. Our "covered growth" provides a convenient and effective solution to the mass loss issue of thin films that serve as catalysts for a variety of 2D material syntheses.

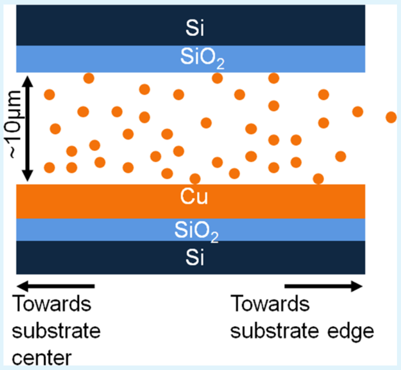

KEYWORDS: *copper, thin film, grain growth, CVD graphene, evaporation*

INTRODUCTION

Of all the materials that can be used to synthesize graphene, copper is the most widely used. Graphene synthesis can occur through many different avenues, ranging from sublimation of SiC to CVD using transition metal foils.[1−6] Copper foil is the most commonly used, but it can lead to deformities in the graphene, during the growth and transfer process.[7] This is a result of many sources of macroscopic deformities, e.g. rolling marks from the manufacturer, scratches from the processing steps, and large wrinkles that can also arise during processing. Metal thin films on silicon wafers afford an improvement over the use of metal foils in terms of rigidity. Having a rigid substrate such as SiO_2/Si also allows the processing of graphene using methods already in place in the semiconductor industry.[8,9]

A practice used in graphene synthesis is to anneal the substrate prior to growth.[10] Annealing increases the grain size of the metal substrate and reduces the amount of surface oxides. However, the use of copper thin films prevents long anneal times compared with foils due to mass loss in evaporation (and possibly dewetting depending on film thickness) within 20 min under low pressure CVD (LPCVD) conditions. There are different methods to reduce the amount of copper lost. One relies on using a copper enclosure around the entire piece.[11] This method would not work on SiO_2/Si pieces due to alloying of copper and silicon. Using our method it would be easier to model gas flow and growth dynamics. The use of an enclosure precludes this method, as each enclosure is not produced in the same manner each time, resulting in process variability. Another method uses a quartz enclosure over the entire piece instead of copper.[12] This is not suitable for scale-up processes, as an ever increasing enclosure would need to be made to support the larger growth substrate. An additional method uses a quartz cover on copper foils.[13] This method has demonstrated a reduction in copper loss, but only for foils, which have higher surface roughness compared to copper films.[14] Adapting this method to copper films allows us to have smooth substrates on which to grow graphene and robust substrates from which we can transfer with minimal concern for introducing additional defects during substrate handling for transfers. We present a method to suppress copper film evaporation under high temperature/vacuum conditions. By suppressing the evaporation, we can reduce defects due to any nonuniformity in the copper film or heating that may arise during growth. This would potentially allow for greater uniformity on wafer scale growth. The new method allows up to 4 h annealing time for the copper film, which addressed the mass loss issue in conventional uncapped growth and yields similar quality for synthesized graphene. With this new synthesis method, we discover that long anneal times do not affect the copper grain size past 60 min and the average graphene domain size growth of graphene is independent of the underlying copper grain size.

Received: September 25, 2014
Accepted: December 31, 2014
Published: December 31, 2014

DOI: 10.1021/am506601v
ACS Appl. Mater. Interfaces 2015, 7, 1527−1532

EXPERIMENTAL METHODS

Copper Film Deposition and Graphene Growth. A 0.8−1.5 μm copper film was deposited using electron-beam evaporation (Plasmaterial, 99.99% pellets) at 10^{-6} Torr on a 300 nm SiO_2/Si wafer. The evaporated copper film sample was loaded with a SiO_2/Si cap directly above and in intimate contact. This stack was annealed in a horizontal hot-wall 1 in. quartz tube furnace under a hydrogen flow rate of 2 sccm at a temperature of 1000 °C and pressure of 2.5×10^{-2} mbar for various times, up to 4 h. For graphene growth, after the annealing step, methane was introduced with a flow rate of 4 sccm for 45 min. After growth, the methane flow rate was increased to 10 sccm and the furnace was cooled from the growth temperature to ambient at a rate of approximately 10 °C/min. The graphene was transferred to SiO_2/Si using the PMMA transfer method outlined elsewhere.[6]

Material Characterization. A Renishaw In-Via Raman Microscope with He−Cd blue laser (442 nm wavelength) was used to observe the quality of graphene grown on the copper film. Copper grain statistical data was acquired from SEM (or OM) images using ImageJ software. Electron back scattering diffraction was performed on an EDAX/TSL OIM collection system attached to a FEI scanning electron microscope and analyzed with an AZTEC digitized inversed pole figure.

Device Fabrication and Characterization. Back-gated field effect transistors (FETs) were made to measure electrical properties via a shadow mask with a CHA e-beam evaporator at 10^{-6} Torr to form 2 nm Ti + 48 nm Au (or Pd) contact pads. By probe-scratching, graphene FETs were isolated from each other with defined channel width equal to the edge of the square metal contact pad (200 μm) and length equal to the gap between them (50, 100, and 200 μm). Electrical characterization was performed on a Cascade probe station with an Agilent 4156 analyzer under ambient conditions, and the typical drain voltage is 20 mV, with gate bias swept from −50 to 50 V. An E-beam evaporated copper film on SiO_2/Si is covered with a piece of SiO_2/Si, with dimensions that are slightly larger than the work-piece.

When cover pieces smaller than the copper film work-piece are used, then the exposed areas of the copper film will still suffer the aforementioned mass loss issue. The entire stack is then placed into a one-inch quartz tube and annealed at 1000 °C for times of up to 4 h. The copper film without a cover underwent evaporation, and after approximately 20 min, it became discontinuous with considerable mass loss, as shown in Figure 1. Graphene has been grown on uncovered copper films, but there is a short time limit (<10 min) before the discontinuities in the copper film make it unusable.[15]

RESULTS AND DISCUSSION

The conditions that are present during LPCVD are similar to that of physical vapor deposition (PVD) for the source (i.e., we have an evacuated chamber [furnace tube], an evaporation source [copper film], and an elevated temperature [annealing/growth temperature]).The cover then acts as a "target" for the metal evaporating from our substrate, "source." Since the same conditions required for PVD have been established, we used the equations that govern evaporation rates for a given pressure to arrive at eq 1, which is derived from Langmuir−Knudsen theory

$$R_{evap} = 5.83 \times 10^{-2} A_s \left(\frac{m}{T}\right)^{1/2} P_e \tag{1}$$

where 5.83×10^{-2} is an amalgam of all of the physical constants, A_s is the source area, m is the gram molecular mass, T is the temperature, and P_e is the vapor pressure.[16] Given our growth conditions, an evaporation rate of 8.0×10^{-7} g/s can be estimated from this equation. Since the films we used are 1.5 μm thick, we had at most 28 min before the entire film evaporated for uncovered growth. For capped growth, the cover piece is at the same temperature as the substrate. This would mean that any copper that evaporated from the substrate would most likely re-evaporate from the cover, leading to a net zero transfer of copper atoms. As graphene grows and slowly covers the copper, a reduction in the evaporation of copper occurs. Copper that might be on the cover piece re-evaporating would end up on the surface of the graphene. This copper would then participate in the back and forth evaporation between the cover piece and graphene surface. The amount of copper that is trapped this way is less than our current detection capabilities. The differences between the covered and uncovered copper film under LPCVD conditions are illustrated in Figure 2a and b. The mean free path for copper atoms during our annealing conditions is 9.6×10^4 μm, which is much greater than the separation between the film and the cover, as shown in Figure 2c. Near the edges of the cover, the copper has a path other than directly on the cover. This results in copper loss near the edges due to diffusion of copper into the quartz tube. As copper is being lost from the edges, it becomes harder to lose more copper due to the increased distance of the exposed copper edges from the open space of the quartz tube. Once the annealing and growth have been completed, the cover itself comes off easily and there is no residual copper on the surface of the cover (Figure S1).

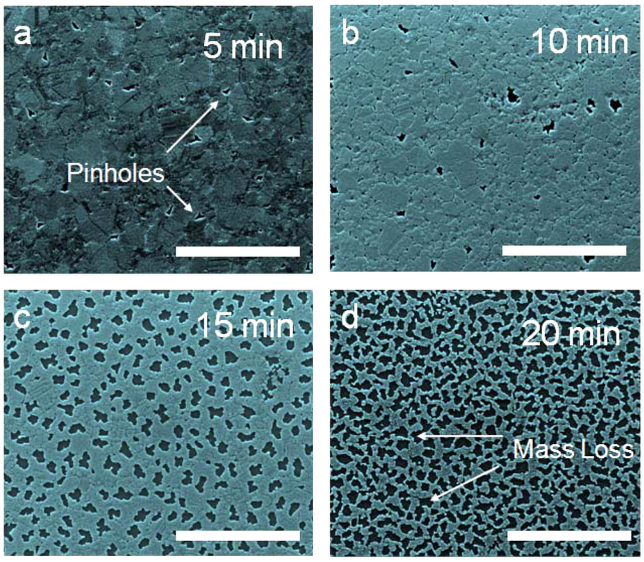

Figure 1. SEM images of the evaporation of copper films (~1 μm thick) as a function of anneal time at 1000 °C. Five minute time increments from a to d. Scale bar is 100 μm. (a) Pinholes appear as grain size increases. Examples of pinhole formation highlighted. (b) Grain size does not appear to increase further, but pinholes become larger as copper film continues to coalese. (c) Density and size of holes increase as film evaporates. (d) Holes in the copper film continue enlarging due to mass loss. Examples of mass loss areas are highlighted.

To demonstrate our hypothesis of trapping copper between a cover to reduce evaporative losses, we took a copper film that, when deposited at room temperature, consists of nanocrystalline copper grains and annealed the samples. The normal growth steps for graphene on a 1 μm thick copper film involve a 5 min anneal, followed by a 5 min growth step. During the 10 min overall processing time that is available without the aid of a cover, the average grain size achieved was approximately 10 μm. With a cover, we substantially increased the amount of time that a copper film can be annealed. Annealing was performed for various time ranges to determine if there is a maximum size

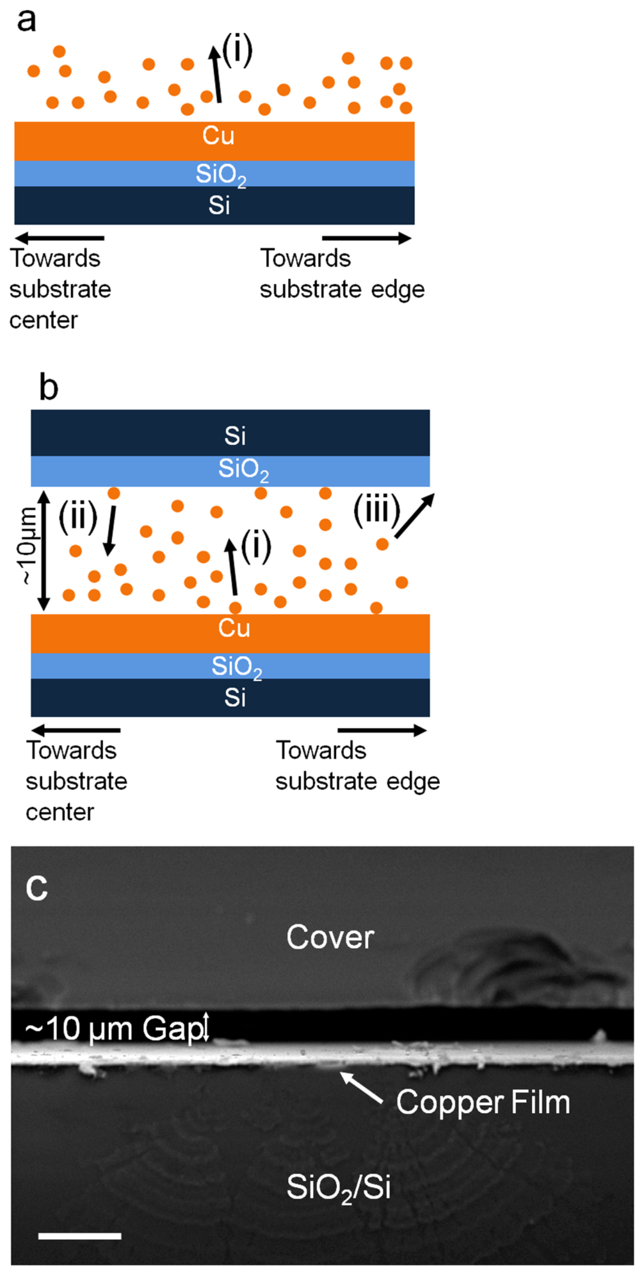

Figure 2. Cartoon illustration of the atomic paths of copper during anneal or growth. (a) In an uncovered copper film the copper is free to evaporate and will condense at any suitable surface. (b) In the covered copper film there are three possible paths. Copper atoms can (i) evaporate from the copper film, (ii) adsorb and then desorb from the cover, or (iii) escape from the edge of the copper film and condense at any suitable surface of the furnace tube, such as an uncovered piece. (c) Cross-sectional SEM image of the gap between the cover and the copper film. The cover has a 300 nm SiO_2 layer to prevent copper alloying with silicon. The mean free path of copper atoms at annealing pressures (2.5×10^{-2} mbar at 1000 °C) is 9.6×10^4 μm. During growth conditions (5.7×10^{-2} mbar at 1000 °C) the mean free path reduces to 2.5×10^4 μm due to an increase in system pressure as methane is admitted into the furnace tube, still orders greater than the cover/film separation. Scale bar is 20 μm.

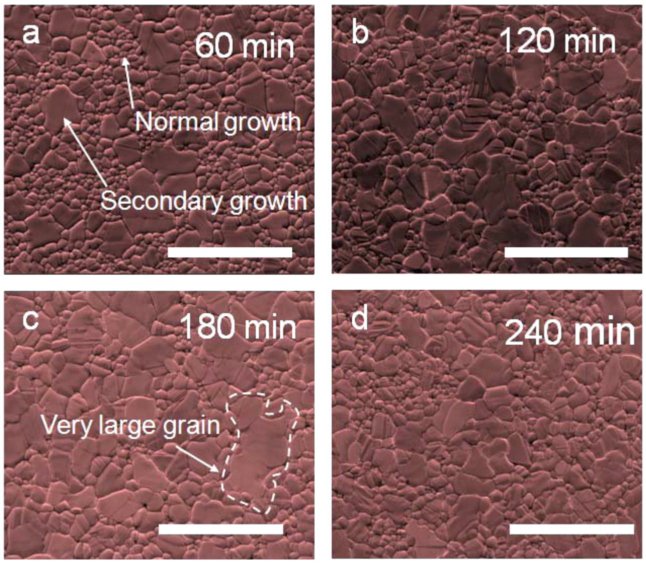

Figure 3. SEM images of a covered 1-μm-thick copper film grain growth as a function of time. One hour time increments from a to d. Scale bar is 100 μm. (a) Grain size has increased with no pinhole formation. (b) Some of the larger grains are approaching 50 μm. (c) Overall grain size does not appear to be increasing further. There are occasional grains with sizes approaching 100 μm. (d) No considerable change in grain distribution from 60 min. There appears to be secondary grain growth from the 60 min point. The grain size distribution for a larger area is shown in Supporting Information (SI) Figure S2.

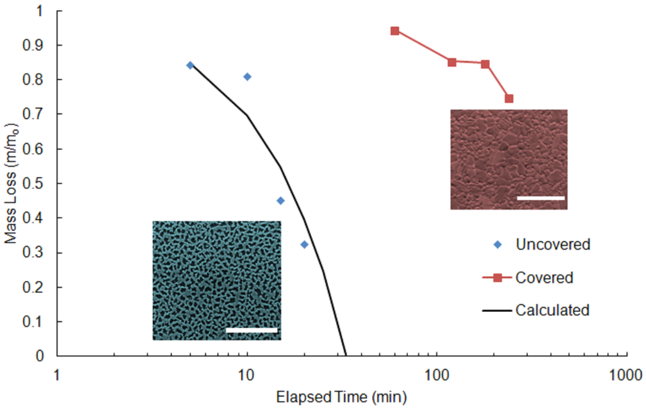

Figure 4. Copper mass loss comparison between uncovered and covered growth substrates. Calculated values based on sample dimensions of 7 mm × 8 mm. Copper mass lost in covered samples does not approach that of uncovered samples until approximately 120 min. At that point most of the grain growth has completed as seen in Figure 3. Inset images correspond to film coverage at maximum anneal times of 20 and 240 min for uncovered and covered samples, respectively. Scale bars are 100 μm.

that the copper grains will reach within a reasonable amount of time. Even at our longest time scale of 4 h, there did not seem to be any visual evidence that there was excessive copper loss. During normal grain growth, grain sizes of metal thin films can reach a size that is comparable to the film thickness. Normal grain growth can be described as the growth of the grains in the thin film up to the point when the film develops a columnar grain structure, i.e. when the grain boundaries intersect both the top and bottom surfaces of the film.[17] When the copper film was covered, we observed copper grains that were larger than normal growth should allow. This would suggest that normal grain growth had stopped and anisotropic grain growth had occurred.[17−19] Anisotropic grain growth occurs when a small subset of the grains continue growth in the lateral direction,

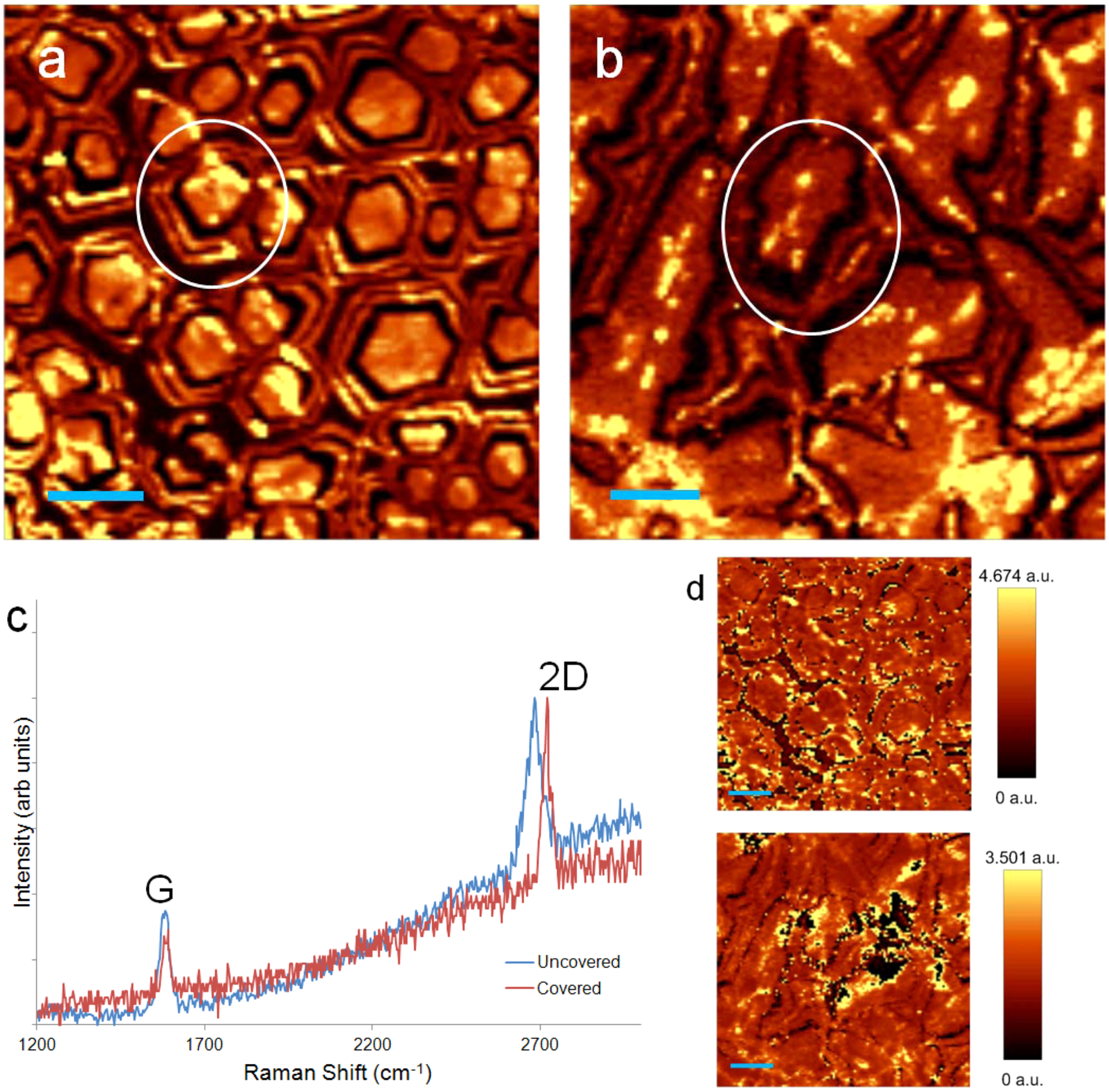

Figure 5. (a) Raman mapping of the G peak of uncovered isotope labeled growth. Normal methane and ^{13}C enriched methane cycled in 1 min increments, starting with normal methane. (b) Covered isotope labeled growth with the G peak mapped. Normal methane and ^{13}C enriched methane cycled in 12 min increments, starting with normal methane. In (a) and (b) bright regions are normal methane and dark areas are ^{13}C enriched methane. A typical graphene domain has been circled. (c) Comparison of typical Raman spectra from uncovered and covered copper films. The fwhm of the 2D peaks are 30 and 32 cm^{-1} for the covered and uncovered films, respectively. (d) I_{2D}/I_{G} ratio for uncovered (5 min growth) and covered (60 min growth) copper films, top and bottom, respectively. The dark regions are the copper grain boundaries. All scale bars are 5 μm.

even though the remaining grains have ceased growth.[17] As shown in Figure 3a the grain size appears to stop normal grain growth after approximately 1 h with larger grains appearing as a result of secondary grain growth. Statistical analysis over an area of 100 × 100 μm^2 does not indicate a bimodal distribution of large and small copper grains (Figure S2). Closer analysis of larger copper grains reveals coalescence occurring even in later time frames.

With the cover in place there is still some loss of copper, but the loss rate is much slower than the loss rate of the uncovered copper film, as seen in Figure 4. The mass loss percentage of the covered copper film approaches that of the uncovered copper film after nearly 90 min versus 5 min for the uncovered film. This indicates that the lifetime of the covered copper film is 16 times higher than that of the uncovered one, under the same process conditions. Leaving the uncovered copper film in the furnace for 1 h would lead to complete loss of the copper film, whereas, with the cover, the copper film has negligible loss. We can see the mass loss tracks with the estimated evaporation rate in eq 1. There is a clear differentiation between the covered and uncovered films; that is, pinhole evolution is obvious in the uncovered film (Figure 1) but not in the covered film due to the mass loss mechanism previously discussed. This allows us to maintain a usable portion of the film near the center using our covered method, whereas with no cover the entire film is no longer viable within the CVD growth time frame. The use of a cover does not change how the crystalline structure of the copper film evolves as it is annealed. The copper film in this growth method still takes on a predominately ⟨111⟩ grain orientation,[17] which is favorable for high-quality graphene growth.[10,20] By having the copper film loss rate greatly suppressed, it would be possible to reduce the film thickness,

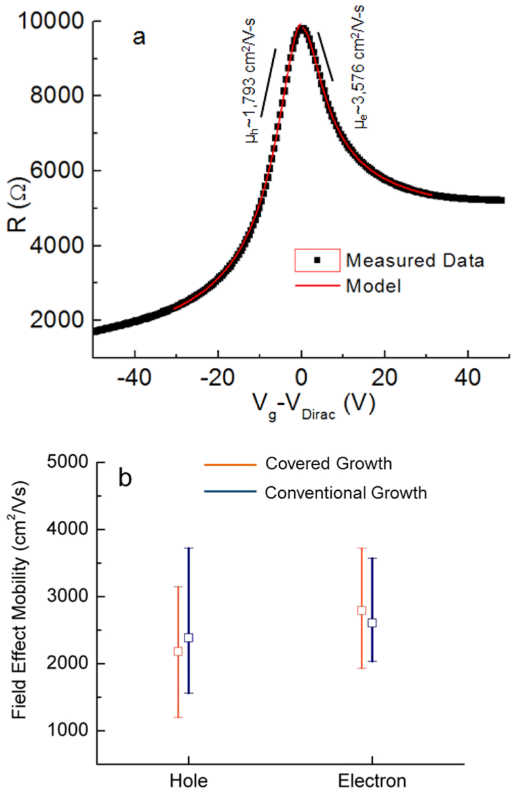

Figure 6. Electrical characterization of the graphene devices made from the two growth methods. (a) Resistance versus gate voltage characteristic with a model fit for a FET device, showing hole and electron mobility of 1,793 and 3,576 $cm^2/V{\cdot}s$ at ambient conditions. (b) Statistical values of field-effect mobility from several devices based on uncovered and covered growth of graphene.

while retaining a uniform film. Since this process is more thickness scalable than uncovered growth, nonuniformities in film thickness would have less impact on reproducible growth. As the anneal time grows, there is an increasing number of crystalline twins that form. For short annealing times there are no or very little twins, but as the time increases the numbers of twins increase (Figure S3). This could be desirable for certain types of growth, such as in the case of graphene ribbons.[21]

To determine how the cover affected the growth kinetics of graphene on a copper film, growth with isotopic precursors was used. The methane to hydrogen ratio was adjusted to determine the nucleation density as well as the growth rate of the individual graphene domains. With a cover there is a reduction of precursor flow onto the copper surface. This should lead to a reduced nucleation density and growth rate, which, with further refinement, would lead to an increase in graphene domain size. As shown in Figure 5a and b, the statistical average of graphene domain size over numerous samples is approximately 5 μm for the uncovered copper film and 10 μm for the covered copper film. We notice that the growth front shifts from a regular hexagon to an irregular polygon growth front. The growth does not seem to be dendritic because we have not observed the growth front to be anything other than straight. There is a reduction in the graphene nucleation density, but it does not approach the reduction found in other works, even when there is large hydrogen to methane ratio.[22,23] There is also a corresponding reduction in the growth rate, as there is a 12× increase in the cycle growth time for the covered copper film for the same apparent growth in the uncovered copper film. The quality of the graphene does not appear to change from the Raman spectroscopy. One metric of determining graphene quality is the presence or lack of a D peak located at ~1350 cm^{-1}. As shown in Figure 5c, there is no indication of a D peak. The fwhm of the peaks from both covered and uncovered may shift from the covered being larger to the uncovered being larger over the graphene sample. Regardless, the fwhm of the peaks is ~30 cm^{-1}, which is indicative of monolayer graphene. By examining the I_{2D}/I_G ratio in Figure 5d, we can observe that the film is uniform and monolayer over the scan area.

To verify the electrical performance, we fabricated field-effect transistors to determine its electrical characteristics. Electrical measurements were performed using a typical setup with a widely used diffusive transport model for mobility extraction.[10,20,24] As shown in Figure 6a, a representative resistance versus back gate bias curve revealed ambipolar behavior with extracted field-effect mobility for hole and electron in a range of 2–3 k $cm^2/V{\cdot}s$ with carrier density around 3.3–3.8 × 10^{11} cm^{-2} on SiO_2/Si at ambient conditions. The electrical property of the covered synthesis is comparable to the same devices made from uncovered graphene (Figure 6b).

CONCLUSION

We have shown a method to greatly increase the available annealing time for copper films. The copper grains of the thin films appear to reach a maximum size and distribution after approximately 1 h with the use of a cover: an increase of 10 times in copper grain size compared to traditional uncovered growth. We have demonstrated that it is feasible to grow graphene even though the cover is in natural contact with the copper film, and the mass loss of copper has been minimized by a factor of 16 with no adverse deposition on the cover. Graphene grown with a cover has similar electrical properties to graphene grown without the cover. The method we have demonstrated allows for more uniformity for scalable graphene synthesis by reducing any deviations that may occur from differences in evaporation rates over the wafer.

ASSOCIATED CONTENT

Ⓢ Supporting Information

Images of copper film before and after annealing, brief statistical analysis of copper film grains after annealing, and EBSD of long anneal time. This material is available free of charge via the Internet at http://pubs.acs.org.

AUTHOR INFORMATION

Corresponding Author

*E-mail: deji@ece.utexas.edu.

Author Contributions

The manuscript was written through contributions of all authors. All authors have given approval to the final version of the manuscript.

Notes

The authors declare no competing financial interest.

ACKNOWLEDGMENTS

We would like to thank Prof. Rodney Ruoff for his support and guidance in this work. This work is supported in part by the National Science Foundation CAREER award (D.A.), the Southwest Academy of Nanoelectronics (SWAN), and the NSF NASCENT NERC Center.

REFERENCES

(1) de Heer, W. A.; Berger, C.; Wu, X.; First, P. N.; Conrad, E. H.; Li, X.; Li, T.; Sprinkle, M.; Hass, J.; Sadowski, M. L.; Potemski, M.; Martinez, G. Epitaxial Graphene. *Solid State Commun.* **2007**, *143* (1–2), 92–100.

(2) Kim, K. S.; Zhao, Y.; Jang, H.; Lee, S. Y.; Kim, J. M.; Kim, K. S.; Ahn, J.-H.; Kim, P.; Choi, J.-Y.; Hong, B. H. Large-Scale Pattern Growth of Graphene Films for Stretchable Transparent Electrodes. *Nature* **2009**, *457* (7230), 706–710.

(3) Kwon, S.-Y.; Ciobanu, C. V.; Petrova, V.; Shenoy, V. B.; Bareño, J.; Gambin, V.; Petrov, I.; Kodambaka, S. Growth of Semiconducting Graphene on Palladium. *Nano Lett.* **2009**, *9* (12), 3985–3990.

(4) Sutter, P. W.; Flege, J.-I.; Sutter, E. A. Epitaxial Graphene on Ruthenium. *Nat. Mater.* **2008**, *7* (5), 406–411.

(5) Coraux, J.; ǸDiaye, A. T.; Busse, C.; Michely, T. Structural Coherency of Graphene on Ir(111). *Nano Lett.* **2008**, *8* (2), 565–570.

(6) Li, X.; Cai, W.; An, J.; Kim, S.; Nah, J.; Yang, D.; Piner, R.; Velamakanni, A.; Jung, I.; Tutuc, E.; Banerjee, S. K.; Colombo, L.; Ruoff, R. S. Large-Area Synthesis of High-Quality and Uniform Graphene Films on Copper Foils. *Science* **2009**, *324* (5932), 1312–1314.

(7) Luo, Z.; Lu, Y.; Singer, D. W.; Berck, M. E.; Somers, L. A.; Goldsmith, B. R.; Johnson, A. T. C. Effect of Substrate Roughness and Feedstock Concentration on Growth of Wafer-Scale Graphene at Atmospheric Pressure. *Chem. Mater.* **2011**, *23* (6), 1441–1447.

(8) Xiangyu, C.; Akinwande, D.; Kyeong-Jae, L.; Close, G. F.; Yasuda, S.; Paul, B. C.; Fujita, S.; Jing, K.; Wong, H. P. Fully Integrated Graphene and Carbon Nanotube Interconnects for Gigahertz High-Speed Cmos Electronics. *IEEE Trans. Electron Devices* **2010**, *57* (11), 3137–3143.

(9) Gao, L.; Ni, G.-X.; Liu, Y.; Liu, B.; Castro Neto, A. H.; Loh, K. P. Face-to-Face Transfer of Wafer-Scale Graphene Films. *Nature* **2014**, *505* (7482), 190–194.

(10) Tao, L.; Lee, J.; Holt, M.; Chou, H.; McDonnell, S. J.; Ferrer, D. A.; Babenco, M. G.; Wallace, R. M.; Banerjee, S. K.; Ruoff, R. S.; Akinwande, D. Uniform Wafer-Scale Chemical Vapor Deposition of Graphene on Evaporated Cu (111) Film with Quality Comparable to Exfoliated Monolayer. *J. Phys. Chem. C* **2012**, *116* (45), 24068–24074.

(11) Jacobberger, R. M.; Arnold, M. S. Graphene Growth Dynamics on Epitaxial Copper Thin Films. *Chem. Mater.* **2013**, *25* (6), 871–877.

(12) Rümmeli, M. H.; Gorantla, S.; Bachmatiuk, A.; Phieler, J.; Geißler, N.; Ibrahim, I.; Pang, J.; Eckert, J. On the Role of Vapor Trapping for Chemical Vapor Deposition (Cvd) Grown Graphene over Copper. *Chem. Mater.* **2013**, *25* (24), 4861–4866.

(13) Chen, S.; Ji, H.; Chou, H.; Li, Q.; Li, H.; Suk, J. W.; Piner, R.; Liao, L.; Cai, W.; Ruoff, R. S. Millimeter-Size Single-Crystal Graphene by Suppressing Evaporative Loss of Cu During Low Pressure Chemical Vapor Deposition. *Adv. Mater. (Weinheim, Ger.)* **2013**, *25* (14), 2062–2065.

(14) Orofeo, C. M.; Hibino, H.; Kawahara, K.; Ogawa, Y.; Tsuji, M.; Ikeda, K.-i.; Mizuno, S.; Ago, H. Influence of Cu Metal on the Domain Structure and Carrier Mobility in Single-Layer Graphene. *Carbon* **2012**, *50*621892196.

(15) Ismach, A.; Druzgalski, C.; Penwell, S.; Schwartzberg, A.; Zheng, M.; Javey, A.; Bokor, J.; Zhang, Y. Direct Chemical Vapor Deposition of Graphene on Dielectric Surfaces. *Nano Lett.* **2010**, *10* (5), 1542–1548.

(16) Plummer, J.; Deal, M.; Griffin, P. *Silicon Vlsi Technology: Fundamentals, Practice and Modeling*; Prentice Hall: 2000.

(17) Thompson, C. V. Grain Growth in Thin Films. *Annu. Rev. Mater. Sci.* **1990**, *20* (1), 245–268.

(18) Zielinski, E. M.; Vinci, R. P.; Bravman, J. C. Effects of Barrier Layer and Annealing on Abnormal Grain Growth in Copper Thin Films. *J. Appl. Phys.* **1994**, *76* (8), 4516–4523.

(19) Simoes, S.; Calinas, R.; Ferreira, P.; Viana, F.; Vieira, M.; Vieira, M. Thermal Stability of Nanocrystalline Copper Thin Films. *Microsc. Microanal.* **2007**, *13* (Supplement S02), 628–629.

(20) Tao, L.; Lee, J.; Chou, H.; Holt, M.; Ruoff, R. S.; Akinwande, D. Synthesis of High Quality Monolayer Graphene at Reduced Temperature on Hydrogen-Enriched Evaporated Copper (111) Films. *ACS Nano* **2012**, *6* (3), 2319–2325.

(21) Hayashi, K.; Sato, S.; Ikeda, M.; Kaneta, C.; Yokoyama, N. Selective Graphene Formation on Copper Twin Crystals. *J. Am. Chem. Soc.* **2012**, *134* (30), 12492–12498.

(22) Kim, D. W.; Kim, Y. H.; Jeong, H. S.; Jung, H.-T. Direct Visualization of Large-Area Graphene Domains and Boundaries by Optical Birefringency. *Nat. Nano* **2012**, *7* (1), 29–34.

(23) Hao, Y.; Bharathi, M. S.; Wang, L.; Liu, Y.; Chen, H.; Nie, S.; Wang, X.; Chou, H.; Tan, C.; Fallahazad, B.; Ramanarayan, H.; Magnuson, C. W.; Tutuc, E.; Yakobson, B. I.; McCarty, K. F.; Zhang, Y.-W.; Kim, P.; Hone, J.; Colombo, L.; Ruoff, R. S. The Role of Surface Oxygen in the Growth of Large Single-Crystal Graphene on Copper. *Science* **2013**, *342* (6159), 720–723.

(24) Kim, S.; Nah, J.; Jo, I.; Shahrjerdi, D.; Colombo, L.; Yao, Z.; Tutuc, E.; Banerjee, S. K. Realization of a High Mobility Dual-Gated Graphene Field-Effect Transistor with Al_2O_3 Dielectric. *Appl. Phys. Lett.* **2009**, *94* (6), 062107–062103.